

Coordination Compounds of Schiff-Base Ligands Derived from Diaminomaleonitrile (DMN): Mononuclear, Dinuclear, and Macrocyclic Derivatives

Mark J. MacLachlan, Murray K. Park, and Laurence K. Thompson*

Department of Chemistry, Memorial University of Newfoundland,
St. John's, Newfoundland, A1B 3X7 Canada

Received March 6, 1996[⊗]

Copper(II) and V^{IV}O complexes of an open chain (1:2) Schiff-base ligand (H₂L1), derived by the template condensation of diaminomaleonitrile (DMN) and salicylaldehyde, and dicopper(II) complexes of (2:2) macrocyclic Schiff-base ligands derived by template condensation of diformylphenols and diaminomaleonitrile, have been synthesized and studied. Structures have been established for the first time for mononuclear Cu(II) and V^{IV}O derivatives of the open chain ligand H₂L1 (1:2), a dinuclear macrocyclic Cu(II) complex derived from a 2:2 macrocyclic ligand (H₂M1), and the half-condensed 1:1 salicylaldehyde ligand (H₂L2). [Cu(L1)] (1) (L1 = C₁₈H₁₀N₄O₂) crystallized in the monoclinic system, space group *P*2₁/*n* (No. 14), with *a* = 11.753(6) Å, *b* = 7.708(5) Å, *c* = 16.820(1) Å, and *Z* = 4. [VO(L1)(DMSO)] (2) crystallized in the orthorhombic system, space group *Pbca* (No. 61), with *a* = 22.534(9) Å, *b* = 23.31(1) Å, *c* = 7.694(5) Å, and *Z* = 8. H₂L2 (C₁₈H₈N₄O) (3) crystallized in the monoclinic system, space group *P*2₁/*c* (No. 14), with *a* = 13.004(6) Å, *b* = 11.441(7) Å, *c* = 7.030(4) Å, and *Z* = 4. [Cu₂(M3)](CH₃COCH₃) (4) (M3 = C₃₂H₂₄N₈O₄) crystallized in the monoclinic system, space group *C*2/*c* (No. 15), with *a* = 38.33(2) Å, *b* = 8.059(4) Å, *c* = 22.67(2) Å, and *Z* = 8. [Cu(L3)(DMSO)] (5) (L3 = C₂₀H₁₄N₂O₄) crystallized in the triclinic system, space group *P*1̄ (No. 2), with *a* = 10.236(4) Å, *b* = 13.514(4) Å, *c* = 9.655(4) Å, and *Z* = 2. 4 results from the unique addition of two acetone molecules to two imine sites in [Cu₂(M1)](ClO₄)₂ (M1 = 2:2 macrocyclic ligand derived from template condensation of DMN and 2,6-diformyl-4-methylphenol). 4 has extremely small Cu–OPh–Cu bridge angles (92.0, 92.8°), well below the expected lower limit for antiferromagnetic behavior, but is still antiferromagnetically coupled ($-2J = 25.2 \text{ cm}^{-1}$). This behavior is associated with a possible antiferromagnetic exchange term that involves the conjugated framework of the macrocyclic ligand itself. The ligand L3 in 5 results from hydrolysis of M1 on recrystallization of [Cu₂(M1)](ClO₄)₂ from undried dimethyl sulfoxide.

Introduction

The ligands used in this study are summarized in Chart 1.

Diaminomaleonitrile (DMN) (Figure 1) results from the polymerization of HCN under basic conditions,¹ and the X-ray structure² is consistent with a molecule having significant carbon–carbon double-bond character (C–C 1.363(6) Å). In 1971 the first complexes of DMN with platinum and palladium salts were reported,³ and the intensely colored derivatives [M(C₄H₂N₄)₂] (M = Ni, Pd, Pt) were formulated as neutral species with various structural representations depending on whether the ligand is assumed to be a neutral diimine derivative, a monoanionic, charge-delocalized species, or a dianionic species (Figure 1a–c, respectively). This would formalize the metal oxidation state as 0, II, or IV, respectively. The platinum complex [Pt(DISN)₂], resulting from the reaction between K₂PtCl₄ and DMN in water, was subsequently shown to be a diiminosuccinonitrile complex,⁴ involving proton loss and formal oxidation of DMN itself. A chemical parallel exists between this system and *o*-phenylenediamine, where the complexes [M(BQDI)₂] (M = Co, Ni, Pd, Pt) are formally complexes of the benzoquinone diimine anion.^{5,6} An interesting observation concerns the products formed by recrystallization of [Pd-

(DMN)₂Cl₂] from acetone and ethyl methyl ketone, which were shown to be Schiff-base adducts, where one ketone condensed on each ligand at one of the NH₂ groups.³

Our interest in this molecule stems from its ability to act as a diamine and form simple Schiff-base ligands but also from the fact that the electron-withdrawing CN groups, which clearly affect the coordinating capacity of DMN itself, have the potential to modulate the electronic properties of resulting coordination complexes and also their chemical reactivity. Condensation of DMN with salicylaldehyde produces just the 1:1 Schiff-base adduct, and in the absence of a metal ion template effect the only way the second condensation step occurs is in the presence of sulfuric acid or phosphorus pentoxide.^{7,8} Template reactions of salicylaldehyde and DMN in the presence of CuCl₂·2H₂O produced inconsistent results, possibly as a result of using acetone for recrystallization in some cases, but the complex [Cu(L1)] (H₂L1 = 2,3-bis((2-hydroxybenzylidene)amino)-2,3-butenedinitrile) (Chart 1) was synthesized successfully from ethanol followed by recrystallization from benzene.⁷ The complexes [M(L1)] (M = Co, Ni) have also been reported,^{9,10} but to our knowledge no structures have been determined.

In this study we report the crystal structures of the complexes [Cu(L1)] and [VO(L1)((CH₃)₂SO)], and the mono-condensed ligand H₂L2 (2-((2-hydroxybenzylidene)amino)-3-amino-2,3-butenedinitrile) (Chart 1). Recrystallization of the macrocyclic

* Corresponding author.

[⊗] Abstract published in *Advance ACS Abstracts*, August 15, 1996.

(1) Gryszkiewics-Trochimowski, E. *Rocz. Chem.* **1928**, 165.

(2) Penfold, P. R.; Lipscomb, W. N. *Acta Crystallogr.* **1961**, 589.

(3) Miles, M. G.; Hursthouse, M. B.; Robinson, A. G. *J. Inorg. Nucl. Chem.* **1971**, 33, 2015.

(4) Lauher, J. W.; Ibers, J. A. *Inorg. Chem.* **1975**, 14, 640.

(5) Balch, A. L.; Holm, R. H. *J. Am. Chem. Soc.* **1966**, 88, 5201.

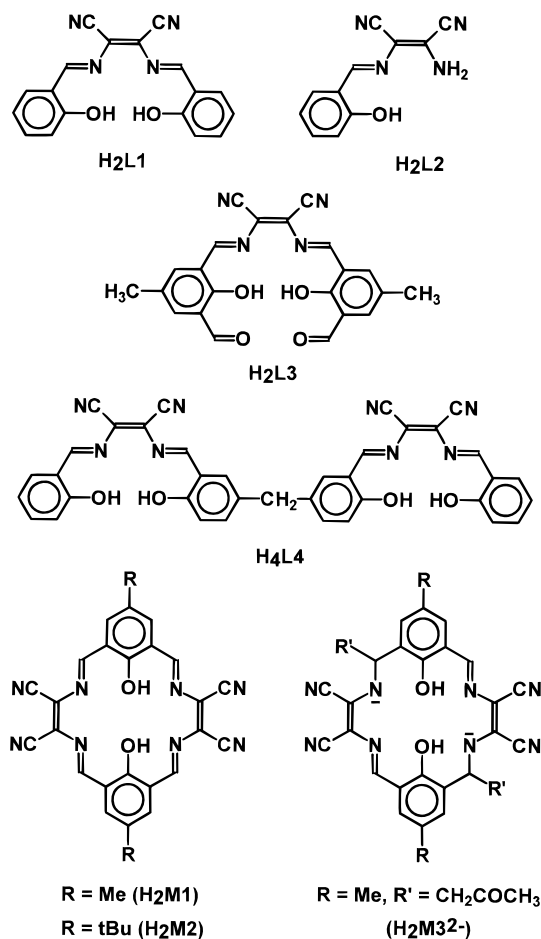
(6) Hall, G. S.; Soderberg, R. H. *Inorg. Chem.* **1968**, 7, 2300.

(7) Iwamoto, T.; Suzuki, H. *Chem. Lett.* **1976**, 343.

(8) Begand, R. W.; Neumer, J. F. U.S. Patents 3,912,274 and 3,914,726, 1975.

(9) Wöhrle, D.; Buttner, P. *Polym. Bull.* **1985**, 13, 57.

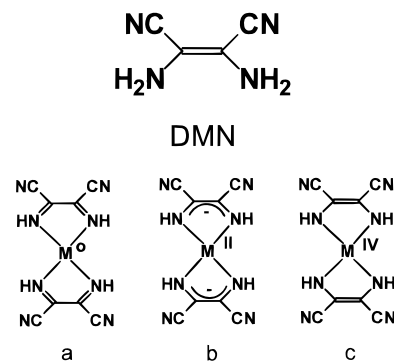
(10) Wöhrle, D.; Bohlen, H.; Rothkopf, H.-W. *Makromol. Chem.* **1983**, 184, 763.

Chart 1. Ligands Derived from Diaminomaleonitrile (DMN)

complex $[\text{Cu}_2(\text{M1})](\text{ClO}_4)_2^{11}$ ($\text{H}_2\text{M1}$, Chart 1) from acetone results in the formation of the neutral complex $[\text{Cu}_2(\text{M3})](\text{CH}_3\text{COCH}_3)$, containing the deprotonated macrocyclic diacetyl ligand M3^{4-} (Chart 1), which is formed by addition of two acetone molecules across two imine groups. A crystal structure for this compound is also reported. This complex has the smallest Cu–Cu distance (2.79 Å) and Cu–OPh–Cu angles (92.0, 92.8°) for any complex of this sort. Magnetic data indicate this complex to be antiferromagnetically coupled, despite the fact that the oxygen bridge angles are well below the expected limiting angle for such behavior.^{12–14} Recrystallization of $[\text{Cu}_2(\text{M1})](\text{ClO}_4)_2$ from undried dimethyl sulfoxide causes hydrolysis of the macrocyclic ligand, forming the dicarboxaldehyde complex $[\text{Cu}(\text{L3})(\text{DMSO})]$, the structure of which is also reported. A dinuclear copper(II) complex of $\text{H}_2\text{L2}$ and an extended dinuclear copper(II) complex of $\text{H}_4\text{L4}$ (Chart 1), a ligand in which two $\text{H}_2\text{L1}$ ligands are joined at the 4-position via a methylene linkage, are also reported.

Experimental Section

Physical Measurements. Electronic spectra were recorded as Nujol mulls and in solution using a Cary 5E spectrometer. Infrared spectra were recorded as Nujol mulls using a Mattson Polaris FT-IR instrument. Microanalyses (C, H, N) were carried out by Canadian Microanalytical

**Figure 1.** Structural representations for DMN and its complexes.

Service, Delta, Canada, and copper analyses by atomic absorption spectroscopy (Varian Techtron AA-5). ESR spectra were measured using a Bruker ESP 300 spectrometer, and electrochemical data were obtained with a BAS CV27 voltammograph. Room-temperature magnetic susceptibilities were measured by the Faraday method using a Cahn 7600 Faraday magnetic balance, and variable-temperature magnetic data (4–305 K) were obtained using an Oxford Instruments superconducting Faraday susceptometer with a Sartorius 4432 microbalance. A main solenoid field of 1.5 T and a gradient field of 10 T m^{-1} were employed.

Safety Note! Perchlorate complexes are potentially explosive, and caution should be exercised when such derivatives are handled. However, the small quantities used in this study were not found to present a hazard. In our laboratory, small quantities of perchlorate complexes are routinely tested for their explosive potential by controlled mechanical impact.

[Cu(L1)] (1) and [VO(L1)] (2). $\text{Cu}(\text{NO}_3)_2 \cdot 3\text{H}_2\text{O}$ (0.507 g, 2.10 mmol) and salicylaldehyde (0.514 g, 4.21 mmol) were dissolved together in refluxing methanol (175 mL) to give a clear green solution. DMN (0.229 g, 2.12 mmol), dissolved in methanol (25 mL), was added dropwise and refluxing continued for 4 h. The intense red-purple solution deposited a deep purple solid, which was filtered off, washed with methanol, and dried under vacuum (yield 96%). Recrystallization from toluene gave purplish-blue crystals suitable for X-ray analysis. Anal. Calcd for $[\text{Cu}(\text{C}_{18}\text{H}_{10}\text{N}_4\text{O}_2)]$ (1): C, 57.22; H, 2.67; N, 14.83. Found: C, 57.15; H, 2.76; N, 14.81. **2** was synthesized in a similar manner using $\text{VO}(\text{SO}_4) \cdot 2\text{H}_2\text{O}$ to give reddish brown crystals, which were filtered off, washed with methanol, and dried under vacuum. Anal. Calcd for $[\text{VO}(\text{C}_{18}\text{H}_{10}\text{N}_4\text{O}_2)]$ (2): C, 56.71; H, 2.64; N, 14.70. Found: C, 56.45; H, 2.65; N, 14.80. Recrystallization from DMSO gave red crystals suitable for X-ray analysis.

H₂L2 (3). Salicylaldehyde (0.580 g, 4.75 mmol) and DMN (0.503 g, 4.65 mmol) were added to absolute ethanol (100 mL), and the mixture was refluxed for 16 h. The resulting yellow solution was cooled in ice to give fine yellow needles, which were filtered off, washed with ethanol, and dried under vacuum. Yield: 0.35 g (35%). Anal. Calcd for $\text{C}_{11}\text{H}_8\text{N}_4\text{O}$ (3): C, 62.26; H, 3.77; N, 26.40. Found: C, 61.99; H, 3.83; N, 26.16. Red crystals suitable for X-ray analysis were obtained by slow evaporation of a methanol solution.

[Cu₂(M3)]·CH₃COCH₃ (4). $[\text{Cu}_2(\text{M1})](\text{ClO}_4)_2^{11}$ which is deep purplish brown, was recrystallized from acetone to give an orange-brown crystalline solid suitable for X-ray analysis. Anal. Calcd for $[\text{Cu}_2(\text{C}_{35}\text{H}_{30}\text{N}_8\text{O}_5)]$ (4): C, 54.61; H, 3.93; N, 14.56. Found: C, 54.38; H, 4.06; N, 14.24.

[Cu(L3)((CH₃)₂SO)] (5). $[\text{Cu}_2(\text{M1})](\text{ClO}_4)_2$ was recrystallized from undried dimethyl sulfoxide to give red crystals of **5** suitable for X-ray analysis. Anal. Calcd for $[\text{Cu}(\text{C}_{22}\text{H}_{14}\text{N}_4\text{O}_4)(\text{C}_2\text{H}_6\text{SO})]$ (5): C, 53.38; H, 3.73; N, 10.37. Found: C, 53.61; H, 3.70; N, 10.69.

[Cu(L2)₂] (6). $[\text{Cu}(\text{OAc})_2] \cdot 2\text{H}_2\text{O}$ (0.550 g, 1.38 mmol) was dissolved in methanol (50 mL) with stirring and refluxing. $\text{H}_2\text{L2}$ (0.584 g, 2.75 mmol) dissolved in methanol (75 mL) was then added and the mixture refluxed for 11 h to give a khaki-brown precipitate, which was filtered off, washed with methanol, and dried under vacuum. Yield: 0.72 g (96%). Anal. Calcd for $[\text{Cu}(\text{C}_{11}\text{H}_6\text{N}_4\text{O})_2]$ (6): C, 48.26; H, 2.21; N, 20.47; Cu, 23.21. Found: C, 47.90; H, 2.45; N, 20.12; Cu, 22.84.

(11) Thompson, L. K.; Mandal, S. K.; Tandon, S. S.; Bridson, J. N.; Park, M. K. *Inorg. Chem.* **1996**, *35*, 3117.

(12) Crawford, V. H.; Richardson, H. W.; Wasson, J. R.; Hodgson, D. J.; Hatfield, W. E. *Inorg. Chem.* **1976**, *15*, 2107.

(13) Hay, P. J.; Thibeault, J. C.; Hoffmann, R. J. *Am. Chem. Soc.* **1975**, *97*, 4884.

(14) Kahn, O. *Inorg. Chim. Acta* **1982**, *62*, 3.

Table 1. Summary of Crystallographic Data for [Cu(L1)] (**1**), [VO(L1)((CH₃)₂SO)] (**2**), H₂L2 (**3**), [Cu₂(M3)](CH₃COCH₃) (**4**), and [Cu(L3)]((CH₃)₂SO)] (**5**)

	1	2	3	4	5
empirical formula	C ₁₈ H ₁₀ N ₄ O ₂ Cu	C ₂₀ H ₁₆ N ₄ O ₄ VS	C ₁₁ H ₈ N ₄ O	C ₃₅ H ₃₀ N ₈ O ₅ Cu ₂	C ₂₄ H ₂₀ N ₄ O ₅ SCu
fw	377.85	459.37	212.21	769.76	540.05
space group	<i>P</i> 2 ₁ / <i>n</i> (No. 14)	<i>Pbca</i> (No. 61)	<i>P</i> 2 ₁ / <i>c</i> (No. 14)	<i>C</i> 2/ <i>c</i> (No. 15)	<i>P</i> 1̄ (No. 2)
<i>a</i> (Å)	11.753(6)	22.534(9)	13.004(6)	38.33(2)	10.236(4)
<i>b</i> (Å)	7.708(5)	23.31(1)	11.441(7)	8.059(4)	13.514(4)
<i>c</i> (Å)	16.820(3)	7.694(8)	7.030(4)	22.67(2)	9.655(4)
α (deg)					104.54(3)
β (deg)	98.72(2)		97.09(5)	105.09(6)	113.60(3)
γ (deg)					82.21(3)
<i>V</i> (Å ³)	1506(1)	4041(5)	1038(2)	6763(7)	1183.7(8)
ρ _{calcd} (g cm ⁻³)	1.666	1.510	1.358	1.512	1.515
<i>Z</i>	4	8	4	8	2
μ (cm ⁻¹)	14.71	6.07	0.87	13.13	10.50
λ (Å)	0.710 69	0.710 69	0.710 69	0.710 69	0.710 69
<i>T</i> (°C)	26	26	26	26	26
<i>R</i> ^a	0.036	0.062	0.045	0.064	0.043
<i>R</i> _w ^b	0.030	0.050	0.038	0.054	0.036

$$^a R = \sum ||F_o| - |F_c|| / \sum |F_o|. \quad ^b R_w = [\sum w(|F_o| - |F_c|)^2 / \sum w F_o^2]^{1/2}.$$

[Cu₂(L4)] (**7**). Methylenebis(4,4'-salicylaldehyde)¹⁵ (0.340 g, 1.33 mmol), Cu(ClO₄)₂·6H₂O (0.480 g, 1.30 mmol), and Cu(OAc)₂·H₂O (0.260 g, 1.30 mmol) were added to methanol (100 mL), and the mixture was refluxed to give a dark green-brown solution. H₂L2 (0.552 g, 2.60 mmol) was added and the mixture refluxed for 10 h. A dark purple-black solid formed, which was filtered off, washed with methanol, and dried under vacuum. Yield: 0.80 g (78%). Anal. Calcd for [Cu₂(C₃₇H₂₆N₈O₄)·CH₃OH (**7**): C, 57.07; H, 3.02; N, 14.01; Cu, 15.90. Found: C, 56.97; H, 2.84; N, 13.86; Cu, 15.59.

Crystallographic Data Collection and Refinement of the Structures. [Cu(L1)] (**1**). The crystals of **1** are dark purple-blue. The diffraction intensities of an approximately 0.15 × 0.05 × 0.40 mm crystal were collected with graphite-monochromatized Mo Kα radiation using a Rigaku AFC6S diffractometer at 26 ± 1 °C and the ω-2θ scan technique to a 2θ_{max} value of 50.1°. A total of 3020 reflections was measured, of which 2876 (*R*_{int} = 0.039) were unique and 1694 were considered significant with *I*_{net} > 2.0σ(*I*_{net}). The intensities of three representative reflections, which were measured after every 150 reflections, remained constant throughout the data collection, indicating crystal and electronic stability (no decay correction was applied). An empirical absorption correction, based on azimuthal scans of several reflections, was applied, which resulted in transmission factors ranging from 0.87 to 1.00. The data were corrected for Lorentz and polarization effects. The cell parameters were obtained from the least-squares refinement of the setting angles of 22 carefully centered reflections with 2θ in the range 21.5–32.4°.

The structure was solved by direct methods.^{16,17} All atoms except hydrogens were refined anisotropically. Hydrogen atoms were optimized by positional refinement, with isotropic thermal parameters set 20% greater than those of their bonded partners at the time of their inclusion. However they were fixed for the final round of refinement. The final cycle of full-matrix least-squares refinement was based on 1694 observed reflections (*I* > 2.00σ(*I*)) and 227 variable parameters and converged with unweighted and weighted agreement factors of *R* = ∑||*F*_o| - |*F*_c|| / ∑|*F*_o| = 0.036 and *R*_w = [∑w(|*F*_o| - |*F*_c||)² / ∑w *F*_o²]^{1/2} = 0.030. The maximum and minimum peaks on the final difference Fourier map correspond to 0.27 and -0.26 electrons Å⁻³ respectively. Neutral-atom scattering factors¹⁸ and anomalous-dispersion terms^{19,20} were taken from the usual sources. All calculations were performed

with the TEXSAN²¹ crystallographic software package using a VAX 3100 work station. Abbreviated crystal data are given in Table 1. Full experimental and crystal data (Table S1), atomic positional parameters (Table S2), anisotropic thermal parameters (Table S3), and complete bond distances and angles (Table S4) are included as Supporting Information.

[VO(L1)((CH₃)₂SO)] (**2**). The data collection and structure solution were carried out by procedures similar to those for **1**. The DMSO molecule is disordered, occupying two positions 180° apart, pivoted around O(4), and in a 2:1 ratio. Hydrogens were placed in calculated positions or located in difference maps, with isotropic thermal parameters set 20% greater than their bonded partners at the time of inclusion. Abbreviated crystal data are given in Table 1. Full experimental and crystal data (Table S1), atomic positional parameters (Table S5), anisotropic thermal parameters (Table S6), and complete bond distances and angles (Table S7) are included as Supporting Information.

H₂L2 (**3**), [Cu₂(M3)](CH₃COCH₃) (**4**), and [Cu(L3)]((CH₃)₂SO)] (**5**). The data collection and structure solution for **3–5** were carried out by procedures similar to those for **1**. Hydrogen atoms were optimized by positional refinement in all cases, with isotropic thermal parameters set 20% greater than those of their bonded partners, at the time of their inclusion. They were fixed for the final round of refinement. Abbreviated crystal data for **3–5** are given in Table 1. Full experimental and crystal data (Table S1), atomic positional parameters (Table S8 (**3**), Table S11 (**4**), Table S14 (**5**)), anisotropic thermal parameters (Table S9 (**3**), Table S12 (**4**), Table S15 (**5**)), and complete bond distances and angles (Table S10 (**3**), Table S13 (**4**), Table S16 (**5**)) are included as Supporting Information.

Results and Discussion

Synthetic Studies. Early studies on ligands derived from DMN and salicylaldehyde focused on the difficulties of obtaining pure complexes and the fact that, in attempts to produce the bis-salicylidene Schiff-base adduct, the 1:1 product (H₂L2) was obtained, unless severe conditions were employed.⁷ Our studies with these systems have confirmed the difficulty of obtaining H₂L1 by simple organic synthesis, but we have succeeded in using template techniques to produce the complexes [M(L1)] (M = Cu(II), V^{IV}O) by refluxing in methanol. However attempts with Mn(II), Fe(II), Gd(III), and Mg(II) salts produced the uncomplexed ligand H₂L2 as the major product. The difficulties in obtaining the pure copper complex in previous work⁷ may be associated with the choice of an appropriate

(15) Marvel, C. S.; Tarköy, N. *J. Am. Chem. Soc.* **1957**, *79*, 6000.

(16) Gilmore, C. J. *J. Appl. Crystallogr.* **1984**, *17*, 42.

(17) Beurskens, P. T. DIRDIF, Technical Report 1984/1; Crystallography Laboratory: Toernooiveld, 6525 Ed Nijmegen, The Netherlands, 1984.

(18) Cromer, D. T.; Waber, J. T. *International Tables for X-ray Crystallography*; Kynoch Press: Birmingham, U.K., 1974; Vol. IV, Table 2.2A.

(19) Ibers, J. A.; Hamilton, W. C. *Acta Crystallogr.* **1974**, *17*, 781.

(20) Cromer, D. T. *International Tables for X-ray Crystallography*; Kynoch Press: Birmingham, U.K., 1974; Vol. IV, Table 2.3.1.

(21) *Texsan-Texray Structure Analysis Package*; Molecular Structure Corp.: The Woodlands, TX, 1985.

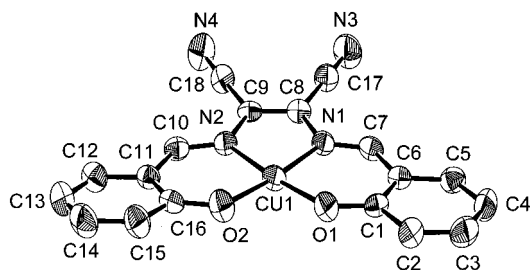


Figure 2. Structural representation for [Cu(L1)] (**1**), with hydrogen atoms omitted (40% probability thermal ellipsoids).

Table 2. Interatomic Distances (Å) and Angles (deg) Relevant to the Copper Coordination Sphere in [Cu(L1)] (**1**)

Cu(1)—O(1)	1.892(3)	Cu(1)—O(2)	1.887(3)
Cu(1)—N(1)	1.950(3)	Cu(1)—N(2)	1.953(3)
C(8)—C(9)	1.338(6)	C(8)—C(17)	1.447(5)
N(1)—C(7)	1.294(5)	C(9)—C(18)	1.440(6)
N(1)—C(8)	1.396(5)	N(2)—C(9)	1.394(5)
N(2)—C(10)	1.309(5)	N(3)—C(17)	1.133(5)
N(4)—C(18)	1.139(5)		
O(1)—Cu(1)—O(2)	89.9(1)	O(1)—Cu(1)—N(1)	93.0(1)
O(1)—Cu(1)—N(2)	175.3(1)	O(2)—Cu(1)—N(1)	174.9(1)
N(1)—C(8)—C(9)	117.2(3)	O(2)—Cu(1)—N(2)	93.1(1)
N(1)—Cu(1)—N(2)	83.8(1)	Cu(1)—O(1)—C(1)	127.6(2)
N(2)—C(9)—C(8)	116.9(4)	Cu(1)—O(2)—C(16)	128.0(3)

solvent for recrystallization. Acetone has been found to react with a dicopper(II) complex of a related ligand H₂M1 (vide supra).

Template condensation of 2,6-diformyl-4(R)-phenols (R = Me, tBu) with DMN in the presence of copper(II) perchlorate in methanol leads to the formation of typical 2:2 macrocyclic complexes [Cu₂(M1)](ClO₄)₂ and [Cu₂(M2)](ClO₄)₂ (see ref 11 and references therein), but only after extended refluxing. Attempts to recrystallize these compounds from methanol, ethanol, DMF, and nitrobenzene led to microcrystalline powders, which corresponded to the unchanged complexes, according to infrared spectra. Large crystals have been obtained by recrystallization from acetonitrile, but they decompose readily by solvent loss and diffract poorly. Recrystallization of [Cu₂(M1)](ClO₄)₂ from acetone, methyl ethyl ketone and 2-acetylpyridine led to a different compound in each case, according to infrared data, with the acetone adduct **4** resulting from the addition of two acetone molecules across two imine linkages in the complexed macrocycle M1²⁻ to form the complexed macrocycle M3⁴⁻. Elemental analysis indicates the incorporation of two acetylpyridine residues in an analogous fashion.

5 results from the recrystallization of [Cu₂(M1)](ClO₄)₂ from dimethyl sulfoxide and is reasonably the result of hydrolytic attack by water, present in the undried solvent, at two adjacent coordinated imine groups, producing the neutral mononuclear dialdehyde complex [Cu(L3)(DMSO)]. The driving force for this reaction could be, in part, the inherent strain in the parent macrocyclic complex but, also, the result of the enhanced electrophilic character at the azomethine carbon centers, associated with the presence of the electron-withdrawing nitrile groups. The same derivative can be prepared by condensing 2,6-diformyl-4-methylphenol and DMN (2:1) in the presence of a copper(II) salt.

Description of the Structures. [Cu(L1)] (**1**). The structure of **1** is illustrated in Figure 2, and bond distances and angles relevant to the copper coordination sphere are listed in Table 2. The structure closely resembles that of [Cu(SALEN)].²² The copper coordination geometry is planar with an angle sum in

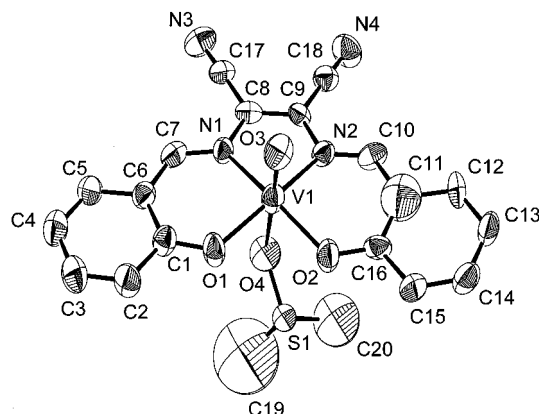


Figure 3. Structural representation for [VO(L1)((CH₃)₂SO)] (**2**), with hydrogen atoms omitted (40% probability thermal ellipsoids).

Table 3. Interatomic Distances (Å) and Angles (deg) Relevant to the Vanadium Coordination Sphere in [VO(L1)((CH₃)₂SO)] (**2**)

V(1)—O(1)	1.965(4)	V(1)—O(2)	1.946(4)
V(1)—O(3)	1.605(5)	V(1)—O(4)	2.327(5)
V(1)—N(1)	2.081(5)	V(1)—N(2)	2.088(5)
C(8)—C(9)	1.358(8)	C(8)—C(17)	1.455(8)
C(9)—C(18)	1.433(9)	N(1)—C(7)	1.309(7)
N(1)—C(8)	1.392(7)	N(2)—C(9)	1.386(7)
N(2)—C(10)	1.313(7)	N(4)—C(18)	1.139(8)
N(3)—C(17)	1.114(8)		
O(1)—V(1)—O(2)	97.1(2)	O(1)—V(1)—O(3)	101.7(2)
V(1)—O(1)—C(1)	128.7(4)	O(1)—V(1)—O(4)	82.2(2)
V(1)—O(2)—C(16)	127.9(4)	O(1)—V(1)—N(1)	89.3(2)
O(1)—V(1)—N(2)	160.7(2)	O(2)—V(1)—O(3)	101.1(2)
O(2)—V(1)—O(4)	83.1(2)	O(2)—V(1)—N(1)	156.8(2)
O(2)—V(1)—N(2)	88.1(2)	O(3)—V(1)—O(4)	173.8(2)
O(3)—V(1)—N(1)	99.3(2)	O(3)—V(1)—N(2)	95.4(2)
O(4)—V(1)—N(1)	75.7(2)	O(4)—V(1)—N(2)	80.1(2)
N(1)—V(1)—N(2)	79.2(2)	N(1)—C(8)—C(9)	118.5(6)
N(2)—C(9)—C(8)	117.2(6)		

the copper plane of 359.8°. Cu(1) is displaced by 0.064 Å from the least-squares N₂O₂ plane (mean deviation of all atoms from the plane is 0.0057 Å). The angle N(2)—Cu(1)—N(1) is small (83.8(1)°) but is the same as that found in [Cu(SALEN)].²² Cu—O bond lengths are slightly shorter in **1**, but other features of the copper coordination sphere are very similar to those of [Cu(SALEN)]. The major difference in the two structures occurs in the dimensions of the Cu—NCCN chelate ring. C—N bond lengths differ significantly. N(2)—C(10) and N(1)—C(7) (1.309(5) and 1.294(5) Å, respectively) are longer than equivalent bonds in [Cu(SALEN)] (1.271(4) and 1.273(4) Å, respectively), while N(2)—C(9) and N(1)—C(8) (1.394(5) and 1.396(5) Å, respectively) are significantly shorter than equivalent bonds in [Cu(SALEN)] (1.460(4) and 1.474(4) Å respectively). The C(8)—C(9) double bond (1.338(6) Å) is much shorter than the [Cu(SALEN)] C—C bond (1.533(5) Å), as would be expected. A comparison of the dimensions of the condensed DMN fragment with DMN itself² reveals very similar bond lengths, in particular in the olefinic and nitrile fragments. However the angles around C(8) and C(9) change dramatically as a result of ligand chelation with the olefinic N—C=C angles in DMN (123.5, 124.8°) being much larger than those in **1** (116.9, 117.2°). Despite this, the hybridization at C(8) and C(9) remains largely unaffected.

[VO(L1)((CH₃)₂SO)] (**2**). The structure of **2** is illustrated in Figure 3, and bond distances and angles relevant to the vanadium coordination sphere are listed in Table 3. The vanadium center is six-coordinate with a rather distorted octahedral structure. The dominant disordered DMSO molecule is shown in Figure 3. The bond angles around the vanadium

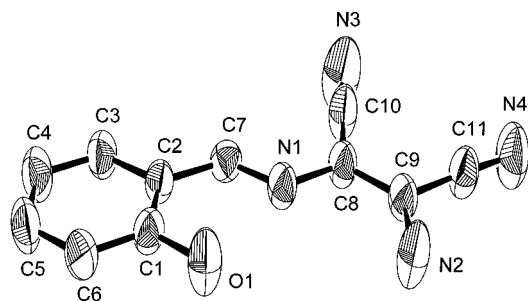


Figure 4. Structural representation for H_2L_2 (**3**), with hydrogen atoms omitted (40% probability thermal ellipsoids).

Table 4. Interatomic Distances (Å) and Angles (deg) in H_2L_2 (**3**)

O(1)–C(1)	1.368(3)	N(1)–C(7)	1.293(3)
C(2)–C(7)	1.452(4)	N(1)–C(8)	1.399(4)
N(2)–C(9)	1.345(4)	N(3)–C(10)	1.139(4)
N(4)–C(11)	1.136(4)	C(8)–C(9)	1.363(4)
C(8)–C(10)	1.437(4)	C(9)–C(11)	1.446(4)
C(7)–N(1)–C(8)	119.4(3)	N(1)–C(7)–C(2)	122.6(3)
N(1)–C(8)–C(9)	119.4(3)	N(1)–C(8)–C(10)	121.8(3)
C(9)–C(8)–C(10)	118.8(3)	N(2)–C(9)–C(8)	126.8(3)
N(2)–C(9)–C(11)	114.2(3)	C(8)–C(9)–C(11)	119.0(3)
N(3)–C(10)–C(8)	177.9(4)	N(4)–C(11)–C(9)	176.1(4)

center fall in the range $75.7\text{--}101.7^\circ$. The $V=O$ bond distance (1.605(5) Å) and the in-plane $V-O$ distances (1.965(4) Å (O(1)), 1.946(4) Å (O(2)) are comparable with those found in the analogous six-coordinate derivative [VO(SALPN)(DMSO)], involving a propane bridge between the two salicylaldimine units.²³ However, in the case of the five-coordinate complex [VO(SALEN)], comparable distances are somewhat shorter.²⁴ The axial $V-O(4)$ (DMSO) distance (2.327(5) Å) is slightly longer than that in [VO(SALPN)(DMSO)].

The dimensions within the five-membered chelate ring encompassing the DMN fragment are very similar to those in [Cu(L1)], implying that the presence of a different metal has done little to change the state of hybridization within the $N-C=C-N$ framework and that the imine $C=N$ and olefinic $C=C$ characters remain largely intact.

H_2L_2 (3**).** The structure of **3**, the half-condensed ligand, is illustrated in Figure 4, and important bond distances and angles are listed in Table 4. The DMN fragment bears a close resemblance to that in DMN itself,² with an identical $C=C$ bond distance (1.363(4) Å). **3** is essentially flat, partly as a result of a hydrogen-bonding interaction between the phenolic hydrogen H(10) and N(1) ($N(1)-H(10)$ distance 1.74 Å and $N(1)-H(10)-O(1)$ angle 152.4°). In addition, the flat nature of H_2L_2 would perhaps be expected as a result of extended π -conjugation to the peripheral nitriles. A slight lengthening of the $C-N$ bond $C(8)-N(1)$ (1.399(4) Å) over $C(9)-N(2)$ (1.345(4) Å) is consistent with the Schiff-base condensation at N(1) and is similar to that observed for both $C-N$ bonds in **1** and **2**.

$[Cu_2(M3)](CH_3COCH_3)$ (4**).** The structure of **4** is illustrated in Figure 5, and bond distances and angles relevant to the copper coordination spheres are listed in Table 5. This complex has a unique structure as a result of the addition of the two acetone molecules to two of the imine linkages in the macrocyclic ligand M1. The structural representation in Figure 5 gives the mistaken impression that the macrocyclic complex is flat but shows that the two acetyl groups, bonded to C(8) and C(18), are projected onto the same face of the molecule. While C(8) and C(18) are

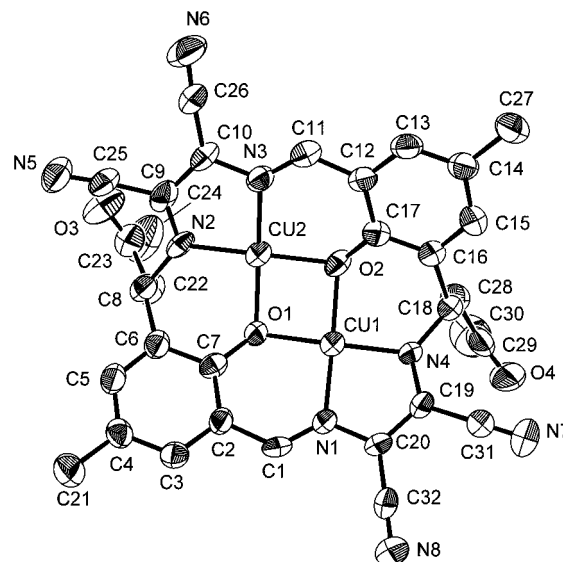


Figure 5. Structural representation for $[Cu_2(M3)]((CH_3)_2CO)$ (**4**), with hydrogen atoms omitted (40% probability thermal ellipsoids).

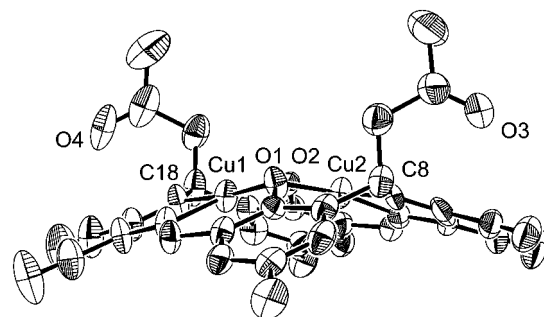


Figure 6. Structural representation for $[Cu_2(M3)]((CH_3)_2CO)$ (**4**) showing the convex shape and the projection of the acetyl groups, with hydrogen atoms omitted (40% probability thermal ellipsoids).

Table 5. Interatomic Distances (Å) and Angles (deg) Relevant to the Copper Coordination Spheres in $[Cu_2(M3)](CH_3COCH_3)$ (**4**)

Cu(1)–Cu(2)	2.788(2)	Cu(1)–O(1)	1.905(5)
Cu(1)–O(2)	1.942(5)	Cu(1)–N(1)	1.913(7)
Cu(1)–N(4)	1.886(6)	Cu(2)–O(1)	1.970(5)
Cu(2)–O(2)	1.908(5)	Cu(2)–N(2)	1.878(6)
Cu(2)–N(3)	1.917(7)		
Cu(2)–Cu(1)–O(1)	44.9(2)	Cu(1)–Cu(2)–N(3)	133.7(2)
Cu(2)–Cu(1)–O(2)	43.1(2)	O(1)–Cu(2)–N(2)	94.5(3)
Cu(2)–Cu(1)–N(1)	132.8(2)	O(1)–Cu(2)–N(3)	170.0(3)
Cu(2)–Cu(1)–N(4)	135.5(2)	O(2)–Cu(2)–N(2)	175.8(3)
O(1)–Cu(1)–O(2)	85.5(2)	O(2)–Cu(2)–N(3)	95.9(3)
O(1)–Cu(1)–N(1)	95.5(3)	N(2)–Cu(2)–N(3)	85.7(3)
O(1)–Cu(1)–N(4)	174.1(3)	Cu(1)–O(1)–Cu(2)	92.0(2)
O(2)–Cu(1)–N(1)	167.1(3)	Cu(1)–O(1)–C(7)	124.0(5)
O(2)–Cu(1)–N(4)	93.5(3)	Cu(2)–O(1)–C(7)	119.7(5)
N(1)–Cu(1)–N(4)	86.8(3)	Cu(1)–O(2)–Cu(2)	92.8(2)
Cu(1)–Cu(2)–O(1)	43.1(1)	Cu(1)–O(2)–C(17)	120.9(5)
Cu(1)–Cu(2)–O(2)	44.1(2)	Cu(2)–O(2)–C(17)	124.0(5)
Cu(1)–Cu(2)–N(2)	136.1(2)		

nominally asymmetric centers, the projection in Figure 6 illustrates a preference for a *cis* configuration, in a structure which is severely bent along the $O(1)-O(2)$ axis (151.1° between the N_2O_2 mean coordination planes and angle sums of 335.7 and 337.7° at O(1) and O(2), respectively). This results in a saucer-like shape with the six-membered chelate rings $Cu(1)-N(4)-C(18)-C(16)-C(17)-O(2)$ and $Cu(2)-N(2)-C(8)-C(6)-C(7)-O(1)$ having boat structures and the 2-oxopropyl groups oriented above the convex face of the molecule. The dinuclear center has the smallest dimensions of any macrocyclic complex of this sort, with a $Cu-Cu$ separation of

(23) Root, A. C.; Hoeschele, J. D.; Cornman, C. R.; Kampf, J. W.; Pecoraro, V. L. *Inorg. Chem.* **1993**, *32*, 3855.

(24) Riley, P. E.; Pecoraro, V. L.; Carrano, C. J.; Bonadies, J. A.; Raymond, K. N. *Inorg. Chem.* **1986**, *25*, 154.

2.788(2) Å and Cu–O–Cu angles of 92.0(2) and 92.8(2)°. Comparable complexes with two-membered linker groups between the phenolic fragments, which would form five-membered chelate rings, are rare and have much larger dinuclear center dimensions. The essentially flat complex [Cu₂-(M4)(H₂O)₂](BF₄)₂ (H₂M4 = macrocyclic ligand formed by template condensation of 2,6-diacetyl-4-methylphenol with ethylenediamine) has a Cu–Cu separation of 2.997(3) Å and a Cu–OPh–Cu angle of 98.8(4)°,¹¹ with a basal ligand array at each copper which is almost planar. The sum of the angles at the oxygen bridge (357.0°) in this compound indicates only minor distortion of the dinuclear center along the O–O (phenoxide) axis. No examples of structures with C₂ olefinic linker groups exist, but systems with *o*-phenylene linkers have comparable dimensions and are essentially flat. A series of complexes with C₆H₄ and C₆F₄ linkers between the phenolic groups have Cu–Cu separations in the range 2.886–2.940 Å and Cu–OPh–Cu angles in the range 97.9–100.9°.²⁵

The severe distortion in **4**, compared with the “flat” structures of comparable dinuclear complexes and the flat structure of **1**, warrants a close examination of the structural features of the DMN fragments in both molecules. The bond lengths and angles in **1** are consistent with a normal tautomeric arrangement within the C(7)–N(1)–C(8)–C(9)–N(2)–C(10) fragment. The C(10)–N(2), C(9)–C(8), and N(1)–C(7) bond distances (1.309(5), 1.338(6), and 1.294(5) Å, respectively) indicate essentially double-bond character for these groups, as would be expected. The comparable fragments in **4** are very different. The angle sums at C(9), C(10), C(19), and C(20) are in the range 359.4–360.0°, clearly indicating trigonal planar centers and flat N–C–C–N chelating frameworks, but the bond lengths indicate a shift in the tautomeric structure. N(2)–C(9) (1.29(1) Å) and N(4)–C(19) (1.33(1) Å) now have significant double-bond character, while C(9)–C(10) (1.42(1) Å) and C(19)–C(20) (1.38(1) Å) have significant single-bond character. In keeping with this, C(8)–N(2) (1.49(1) Å) and C(18)–N(4) (1.53(1) Å) are single bonds, resulting from the acetone addition. N(1)–C(1) (1.278(9) Å) and N(3)–C(11) (1.302(9) Å) are still double-bonded imine groups, as would be expected.

C(10) and C(20) are trigonal planar carbon atoms surrounded by bonds with mostly single-bond character. The complex is neutral, with the ligand having four negative charges. The peculiar hybridization around C(10) and C(20) suggests that significant negative charge resides on these atoms, but it seems more reasonable to assume that delocalization of the anionic charge occurs over the N(2)–C(9)–C(10)–C(26)–N(6) and N(4)–C(19)–C(20)–C(32)–N(8) frameworks. This is supported by the relatively short copper–nitrogen distances (Cu(1)–N(4) 1.886(6) Å; Cu(2)–N(2) 1.878(6) Å).

[Cu(L3)((CH₃)₂SO)] (5). The structure of **5** is illustrated in Figure 7, and bond distances and angles relevant to the copper coordination sphere are listed in Table 6. The copper atom is square-pyramidal with an axially bound DMSO (Cu(1)–O(5) 2.457(4) Å). The CuN₂O₂ coordination plane resembles that in **1**, with comparable Cu–N bond lengths, but slightly longer Cu–O distances. This is probably a consequence of the pyramidal nature of the structure and the slight displacement of Cu(1) toward O(5) (Cu(1) 0.080 Å above the mean basal N₂O₂ plane). The dimensions of the DMN fragment are very similar to those in **1**, indicating a normal tautomeric structure and essentially localized C=C and C=N double bonds.

Spectral, Mechanistic, and Magnetic Properties. Infrared spectroscopy has been a very useful technique for assessing the

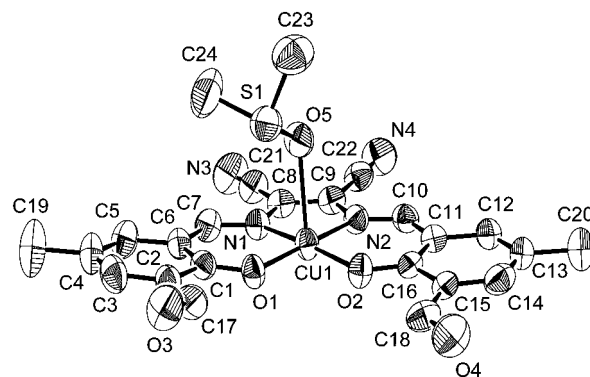


Figure 7. Structural representation for [Cu(L3)((CH₃)₂SO)] (**5**), with hydrogen atoms omitted (40% probability thermal ellipsoids).

Table 6. Interatomic Distances (Å) and Angles (deg) Relevant to the Copper Coordination Sphere in [Cu₂(L3)((CH₃)₂SO)] (**5**)

Cu(1)–O(1)	1.909(3)	Cu(1)–O(2)	1.912(3)
Cu(1)–N(1)	1.959(4)	Cu(1)–N(2)	1.954(4)
C(8)–C(9)	1.359(6)	Cu(1)–O(5)	2.457(4)
C(9)–C(22)	1.448(7)	C(8)–C(21)	1.436(7)
N(1)–C(8)	1.385(6)	N(1)–C(7)	1.302(6)
N(2)–C(10)	1.305(6)	N(2)–C(9)	1.393(6)
N(4)–C(22)	1.119(6)	N(3)–C(21)	1.126(6)
O(1)–Cu(1)–O(2)	90.6(1)	O(1)–Cu(1)–N(1)	92.7(2)
O(1)–Cu(1)–N(2)	175.0(2)	O(2)–Cu(1)–N(1)	172.8(2)
O(2)–Cu(1)–N(2)	93.1(2)	N(1)–Cu(1)–N(2)	83.3(2)
N(2)–C(9)–C(8)	116.9(4)	N(1)–C(8)–C(9)	116.2(4)

outcome of these Schiff-base condensation reactions. DMN itself has major NH stretches at 3440, 3347, and 3206 cm⁻¹ and a strong CN stretching band at 2213 cm⁻¹, with a sharp, weaker shoulder at 2167 cm⁻¹, while the half-condensed ligand H₂L2 has three similar, sharp NH stretches and two ν_{CN} bands, with one at very high energy (2245 cm⁻¹) (Table 7). [Cu(L1)] (**1**) shows no ν_{NH} absorption but a major ν_{CN} stretch at 2222 cm⁻¹, with a weak shoulder at 2172 cm⁻¹. [VO(L1)] (**2**) has an almost identical spectrum in this region, with a single ν_{CN} band at 2222 cm⁻¹. The macrocyclic complex **4** has one strong CN band at 2173 cm⁻¹, with a very weak high-energy shoulder, and two ν_{CO} bands at 1694 and 1712 cm⁻¹ associated with the two different acetone fragments. No perchlorate bands are observed. **5** shows no NH bands, one CN band at 2222 cm⁻¹, and a carbonyl stretch at 1678 cm⁻¹ associated with the aldehyde groups.

6 has a strong ν_{CN} band at 2195 cm⁻¹, with a very weak high-energy shoulder, but a single sharp NH band appears at 3299 cm⁻¹, indicating that just one type of NH proton is present. This complex was synthesized from H₂L2 and copper(II) acetate, and the elemental analysis, coupled with the very low magnetic moment (0.79 μ_B) (Table 7), suggests a dimeric structure (Figure 8) in which two protons are lost, one from the NH₂ group in each H₂L2 ligand. The acidity of this NH proton is reasonably explained by a cyanide inductive effect. **7** has no NH bands, no perchlorate bands, and a single ν_{CN} stretch at 2222 cm⁻¹, similar to **2** and **5**. Elemental analysis and a normal magnetic moment (1.78 μ_B) suggest a dinuclear structure with two neutral bis(salicyclidene) complex fragments joined by the 4,4'-methylene bridge (Figure 8).

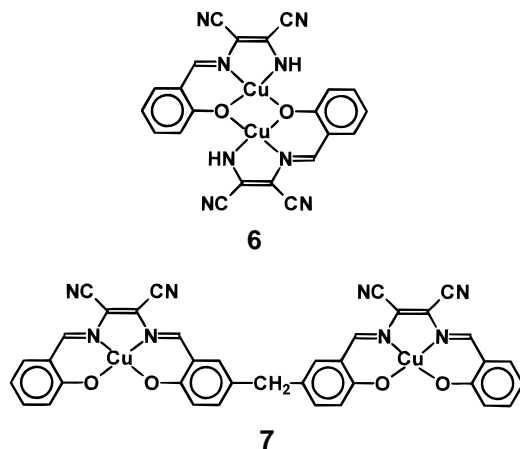
Solutions of all the complexes are highly colored and display intense absorptions in the UV and visible regions. In the region 300–400 nm charge transfer transitions with intensities exceeding 24 000 L·mol⁻¹·cm⁻¹ are observed in all cases except **6**, and in the visible region very intense bands are observed in the range 440–550 nm, which mask any d–d transitions (Table 7). The close similarity between the spectra of **1** and **7** indicates

(25) Brychey, K.; Dräger, K.; Jens, K.-J.; Tilset, M.; Behrens, U. *Chem. Ber.* **1994**, *127*, 465.

Table 7. Spectral and Magnetic Properties^a

compound	ν_{CN} (cm ⁻¹)	UV/vis (nm) (ϵ (L·mol ⁻¹ ·cm ⁻¹))	μ (room temp) (μ_{B})
[Cu(L1)] (1)	2221 (m), 2172 (w)	318 (24 000), 370 (30 100), 388 (31 700), 508 (16 800) ^b	1.85
[VO(L1)] (2)	2222	320 (26 100), 370 sh (27 900), 385 (33 7000), 469 sh (12 300), 518 (15 200) ^b	1.83
H ₂ L2 (3)	2245 (s), 2207 (m)		
[Cu ₂ (M3)][(CH ₃ COCH ₃) (4)	2235 (vw), 2173 (s)	335 (17 500), 390 sh (12 600), 440 (31 000), 480 (15 000) ^c	1.70
[Cu(L3)][(CH ₃) ₂ SO] (5)	2222	370 (15 700), 384 (17 000), 500 (10 600), 550 (10 400) ^c	1.75
[Cu(L2)] ₂ (6)	2236 (vw), 2195 (s)	330 (8100), 360 (6600), 380 (7800), 443 (17 100), 485 (19 300) ^d	0.79
[Cu ₂ (L4)] (7)	2222	274 (38 300), 360 sh (26 900), 377 (35 000), 395 (35 400), 515 (21 700) ^b	1.78
DMN	2213, 2167 (sh)		

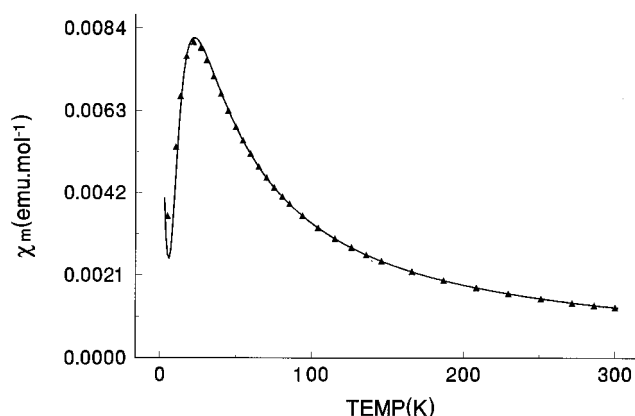
^a ν_{NH} : 3465, 3343, 3188 cm⁻¹ (3); 3299 cm⁻¹ (7); 3440, 3347, 3206 cm⁻¹ (DMN). ^b CHCl₃. ^c DMSO. ^d DMF.

**Figure 8.** Structural representations of [Cu(L2)]₂ (6) and [Cu₂(L4)] (7).

the presence of similar copper chromophores and supports the structural suggestion for this system. The extensive π conjugation present in these systems, coupled with the presence of the electron-withdrawing CN groups, clearly creates an environment for low-energy charge transfer, probably of the $\pi^*-\pi$ type. The anomalous charge transfer situation for **6** in DMF, where the visible bands have much larger intensity than the high-energy bands, clearly sets this compound apart from the others, in keeping with its proposed structure and dianionic ligand.

From a mechanistic viewpoint, the reaction of [Cu₂(M1)]-(ClO₄)₂ with acetone to produce **4** seems unusual, particularly in the absence of any base. However, if the acetone molecules are initially coordinated axially to the copper centers via the carbonyl oxygen, a simple inductive mechanism could be envisaged in which proton dissociation from a methyl group and concomitant enhanced α -carbanion character would lead to intramolecular nucleophilic attack at an adjacent azomethine carbon center. The electrophilic nature of that carbon would also be enhanced by the presence of the adjacent, electron-withdrawing nitrile groups. Molecular models indicate a reasonable fit of acetone in this way. An additional factor which may drive the condensation is the geometric ring strain within the parent macrocyclic complex, resulting from the presence of the small, five-membered DMN based chelate rings, which is clearly relieved in the acetone adduct, based on its high level of distortion.

The acetone addition introduces two chiral centers into the complexed macrocyclic ligand (Figures 5 and 6), and yet only one (cis) stereoisomer is found in the crystal structure. This may result from a process of sequential addition of acetone. The first acetone attaches to an azomethine carbon, creating an sp³ center, which would then produce considerable flexibility in that six-membered chelate ring (it adopts a boat conformation). Accordingly the overall effect would be to allow distortions in other parts of the complexed macrocycle. The

**Figure 9.** Variable-temperature magnetic susceptibility data for [Cu₂(M3)][(CH₃)₂CO] (4). The solid line was calculated from eq 1 with $g = 2.024(3)$, $-2J = 25.2(3)$ cm⁻¹, $\rho = 0.034$, $N\alpha = 57 \times 10^{-6}$ emu, $\Theta = -1.6$ K, $10^2 R = 0.61$ ($R = [\sum(\chi_{\text{obs}} - \chi_{\text{calc}})^2 / \sum\chi_{\text{obs}}^2]^{1/2}$).

resulting saucer-like shape suggests that this distortion would favor the exposure of the other copper(II) center on the same convex face, which would encourage attack of the second acetone on that face (after initial coordination) and in an opposite macrocyclic position.

The room-temperature magnetic moments for **1**, **2**, **5**, and **7** (Table 7) just exceed the spin-only value for a one-unpaired-electron system and are consistent with the mononuclear, one-electron nature of these complexes. Clearly **7** has two isolated single copper sites. **6** has a substantially reduced magnetic moment, consistent with the proposed dimeric, phenoxide-bridged structure (Figure 8), and indicates that the two copper(II) centers are strongly antiferromagnetically coupled.¹¹ **4** has a room-temperature moment which is just less than the spin-only value for copper(II), suggesting the possibility of a spin-coupled system. Variable-temperature susceptibility measurements were carried out on a powdered sample of **4** in the temperature range 4.5–300 K, and the experimental data are illustrated in Figure 9. A sharp maximum in the χ_{m} values at ≈ 30 K indicates rather weak antiferromagnetic coupling, which is confirmed by fitting the data to the Bleaney–Bowers equation (eq 1),²⁶ which is

$$\chi_{\text{m}} = \frac{N\beta^2 g^2}{3k(T - \Theta)} [1 + \frac{1}{3} \exp(-2J/kT)]^{-1} (1 - \rho) + \frac{[N\beta^2 g^2] \rho}{4kT} + N\alpha \quad (1)$$

appropriate for the isotropic exchange Hamiltonian ($H = -2JS_1 \cdot S_2$) for two interacting $S = 1/2$ centers (χ_{m} is expressed per mole of copper atoms, and other terms have their usual meaning). The solid line in Figure 9 corresponds to the best fit of the data to eq 1 with $g = 2.024(3)$, $-2J = 25.2(3)$ cm⁻¹,

(26) Bleaney, B.; Bowers, K. D. *Proc. R. Soc. London* **1952**, *A214*, 451.

$\rho = 0.034$ (paramagnetic impurity fraction), $N\alpha = 57 \times 10^{-6}$ emu, $\Theta = -1.6$ K, and $10^2R = 0.61$. A remarkable feature of this system is the fact that it is still antiferromagnetically coupled, despite the fact that the oxygen (phenoxide) bridge angle is so small.

Experimental observations for dihydroxo-bridged dicopper(II) complexes indicate a changeover from antiferromagnetic to ferromagnetic behavior as the bridge angle falls below 97.5° ,¹² consistent with theoretical calculations which indicate the angle of "accidental orthogonality" to be $\approx 92^\circ$.¹⁴ It is reasonable to assume that a similar situation would prevail for a comparable phenoxide-bridged system. However, when the distortions in the dinuclear center of **4** are considered, the fact that the system is antiferromagnetically coupled, albeit weakly, tends to contradict conventional wisdom. The bending of the dinuclear center along the O(1)–O(2) axis (Figures 5 and 6; 151.1° between the N_2O_2 mean basal planes), coupled with the extreme pyramidal distortion at the phenoxide bridges, would create a situation where antiferromagnetic exchange components would be considerably smaller than expected.^{27,28} Tetrahedral distortion at the copper centers is also responsible for a diminished antiferromagnetic component of total exchange,^{29–31} but in **4** this is not considered to be a factor. Given the small Cu–O–Cu angles in **4**, and the distortions, ferromagnetic coupling would have been predicted. Recent correlations between structure and magnetism for essentially flat macrocyclic complexes related to **4**,¹¹ involving extensive π -conjugation, reveal that a ligand-based antiferromagnetic exchange component is likely to be important to total exchange in systems that possess unsaturated imine linkages and that, at bridge angles where a crossover to ferromagnetism would be anticipated, strong antiferromagnetic coupling still prevails. The persistent but weak antiferromagnetism in **4**, which still retains two imine groups and two π -conjugated pathways linking the metal centers, supports this argument.

Electrochemical studies were carried out on $[Cu_2(M1)](ClO_4)_2$ and $[Cu_2(M2)](ClO_4)_2$ in DMSO, but the cyclic voltammetry for both compounds is very poorly defined, with no discernible reversible or quasi-reversible peaks associated with reduction steps. Although no structural details are yet available for these

compounds, their predicted flat, rigid structures would preclude the flexibility necessary to accommodate the geometric changes likely to accompany copper(II) reduction. This is in sharp contrast to **4**, which has a highly distorted structure and a great deal more flexibility at the copper centers. Two well-defined, almost reversible redox waves are observed in DMSO (GC/SCE/TEAP/DMSO) at $E_{1/2} = -0.57$ and -0.94 V, corresponding to one-electron reduction steps to Cu(II)–Cu(I) and Cu(I)–Cu(I) species, respectively. Comparable redox steps for a similar macrocyclic complex with two reduced imine linkages occur at $E_{1/2} = -0.58$ and -0.90 V, respectively,³² indicating that the remote cyanide groups have a minimal effect on redox potentials. The vanadyl complex **2** exhibits a broad isotropic solid state ESR signal centered at $g = 2.05$ (room temperature), which is resolved in toluene solution to give an eight-line spectrum at room temperature consistent with hyperfine coupling associated with the ^{51}V nucleus ($I = 7/2$). The spectral features are very similar to those observed for [VO(salphen)] (salphen = *o*-phenylenebis(salicylaldimine)), which has a square-pyramidal structure.³³

Conclusion

Structural details are reported for the first time for mononuclear and dinuclear copper(II) complexes and a vanadyl complex of Schiff-base ligands derived from diaminomaleonitrile. These complexes are highly colored, with very intense, low-energy visible absorptions associated with extensive π -conjugation. A unique reaction of a dinuclear macrocyclic complex with acetone leads to addition of two acetone molecules to the macrocyclic ligand to produce a half-saturated diacetyl macrocyclic ligand. The resulting complex displays unprecedented magnetic properties, with persistent antiferromagnetic coupling for very small phenoxide bridge angles.

Acknowledgment. We thank the Natural Sciences and Engineering Research Council of Canada for financial support for this study and Dr. John N. Bridson and David O. Miller for assistance with the X-ray crystallography.

Supporting Information Available: Tables listing detailed crystallographic data, atomic positional parameters, anisotropic thermal parameters, and bond lengths and angles (25 pages). Ordering information is given on any current masthead page.

IC960237P

- (27) Fallon, G. D.; Murray, K. S.; Mazurek, W.; O'Connor, M. J. *Inorg. Chim. Acta* **1985**, *96*, L53.
(28) Charlot, M. F.; Jeannin, S.; Jeannin, Y.; Kahn, O.; Lucrece-Abaul, J.; Martin-Frere, J. *Inorg. Chem.* **1979**, *18*, 1675.
(29) Chiari, P.; Piovesana, O.; Tarantelli, T.; Zanazzi, P. F. *Inorg. Chem.* **1987**, *26*, 952.
(30) Hodgson, D. J. *Inorg. Chem.* **1976**, *15*, 3174.
(31) Sinn, E. *Inorg. Chem.* **1976**, *15*, 366.

- (32) Mandal, S. K.; Thompson, L. K.; Nag, K.; Charland, J.-P. *Inorg. Chem.* **1987**, *26*, 1391.
(33) Wang, X.; Zhang, X. M.; Liu, H. X. *Polyhedron* **1995**, *14*, 293.